Proceedings of the ASME 2019
International Mechanical Engineering Congress and Exposition
IMECE2019
November 11-14, 2019, Salt Lake City, UT, USA

IMECE2019-12182

Brain White Matter Model of Orthotropic Viscoelastic Properties in Frequency Domain

Xuehai Wu and Assimina A. Pelegri[1]

Rutgers, the State University of New Jersey
Piscataway, NJ, USA

John G. Georgiadis

Illinois Institute of Technology
Chicago, IL, USA

ABSTRACT

Finite element analysis is used to study brain axonal injury and develop Brain White Matter (BWM) models while accounting for both the strain magnitude and the strain rate. These models are becoming more sophisticated and complicated due to the complex nature of the BMW composite structure with different material properties for each constituent phase. State-of-the-art studies, focus on employing techniques that combine information about the local axonal directionality in different areas of the brain with diagnostic tools such as Diffusion-Weighted Magnetic Resonance Imaging (Diffusion-MRI). The diffusion-MRI data offers localization and orientation information of axonal tracks which are analyzed in finite element models to simulate virtual loading scenarios.

Here, a BMW biphasic material model comprised of axons and neuroglia is considered. The model's architectural anisotropy represented by a multitude of axonal orientations, that depend on specific brain regions, adds to its complexity. During this effort, we develop a finite element method to merge micro-scale Representative Volume Elements (RVEs) with orthotropic frequency domain viscoelasticity to an integrated macro-scale BWM finite element model, which incorporates local axonal orientation. Previous studies of this group focused on building RVEs that combined different volume fractions of axons and neuroglia and simulating their anisotropic viscoelastic properties. Via the proposed model, we can assign material properties and local architecture on each element based on the information from the orientation of the axonal traces. Consecutively, a BWM finite element model is derived with fully defined both material properties and material orientation. The frequency domain dynamic response of the BMW model is analyzed to simulate larger scale diagnostic modalities such as MRI and MRE.

INTRODUCTION

Axonal stretch can occur when white matter tissue experiences deformation. Given enough stretch, axons can experience irrevocable damage and failure, which leads to further damage from subsequent secondary injury cascades [1, 2,3,4]. Many studies have attempted to identify the constitutive relationship of Brain White Matter (BWM) using finite element methods which aim to sequentially establish injury criteria through the use of actual accident data [2,3,5]. The accuracy of these simulations depends on the correct determination of the material properties and on the precise depiction of the tissues' microstructure [2].

Various material properties and models have been employed in the modeling of BWM. For example, Pelegri's group [2,3] utilized isotropic Ogden hyperelastic material model to model the axonal tortuosity present in the BMW microstructure and to simulate the axonal response to uniaxial tensile stretch. In addition, an approach to generate and implement RVEs with adjustable kinematics which adapted during stretching lead to the development of the transitional kinematic model (TKM). During TKM simulations, "tie" constraints are partially applied to introduce glial couplings for axons with tortuosity varying during the stretching process. Furthermore, periodic boundary conditions are applied to the RVE to mimic the constraint exerting on the RVE by its neighboring RVEs. The TKM [2] yields much better prediction on the tortuosity changes resulting

[1] Contact author: pelegri@rutgers.edu

from uniaxial stretching than the pure affine kinematics model through perfect bonding of axon and glial, and the partially tied model. On another study from the same group [3] an inverse finite element procedure was developed to identify material parameters of spinal cord white matter by combining the results of uniaxial testing with FE modeling. The tortuosity and “tied” constraints from the previous study augmented a pseudo-3D embedded element model a that accounted for multi-axonal interactions. Karami’s group exploited orthotropic viscoelastic material properties in the time domain to model single axons fully coupled to extracellular glial to evaluate time-dependent local stress and strain concentrations. The model used a three-dimensional hexagonal unit cell made of axons and glial which are assumed to be isotropic viscoelastic [6]. The results indicate that the undulation of axons strongly affected the material behavior in the fiber directions, and also the volume fraction (VF) of axons had a much stronger impact on the overall properties of white matter areas. Yuan Feng et al. use experimental data obtained at small strains to identify infinitesimal limits for suitable general functional forms of hyperelastic material models of BWM [7]. As noted, different various material properties have been tested and analyzed for modeling BWM. However, the referenced methods focus on a small part of isolated regions of BWM. They are developing finite element models based on partition methods to separate different sections of BWM to present axons and extracellular glial and present decent results in simplified geometrical structures that consists of multi-axons and extracellular glial. However, in real BWM environment, the tissue architecture between axons and extracellular glial is extremely complicated. Even if one considers only the axonal architecture, that one too is geometrically very complicated for using partition methods in finite element modeling.

On the other hand, the BWM microstructure also contains important information and needs to be considered in the simulations. In the same context, the material orientation can be one key parameter to represent the effect of the complicated BWM microstructure. A lot of studies have utilized the material orientation information in the modeling of BWM [8,9,10,11,12]. For instance, Niall C. Colgan et al. use Diffusion-Weighted Magnetic Resonance Imaging (Diffusion–MRI) to define the orientation of the fibers in BWM to examine diffuse Traumatic Brain Injury (TBI) under high rotational accelerations [8]. R.J.H. Cloots’ group illustrates the strong relationship between the orientations of the microstructure of BWM and axonal injury by simulation of BWM in micro-scale Representative Volume Element (RVE) model [9]. In Margulies et al.’s study, the anatomical detail of the axonal traces in BWM was incorporated into the analysis by computing the oriented axonal strain, rather than by using an anisotropic constitutive model [10]. Sahoo group proposed an implementation of fractional anisotropy to model BWM by considering the mean direction of axonal fiber orientation from Diffusion MRI [11]. Besides the consideration of material orientation of BWM in those studies, the combination of the anisotropic constitutive relationship, material orientation, and related VF information is lacking thus the multi-level BWM simulation is impeded.

In this paper, we developed a new methodology to overcome the traditional drawback of partition methods in finite element modeling of complex structures, such as the one of the BWM, and include material orientation (anisotropic or orthotropic) and appropriate material properties. The tissue level finite element model consists of an assembly of RVEs that exhibit material orientation as sourced from tissues’ microstructure. Thus, few RVE assemblies form a homogenized tissue with constitutive behavior represented by the volume fraction (VF), properties and axonal orientations appropriately coupled to simulate the regional BWM under consideration.

MATERIAL AND METHODS

1. RVE model

A viscoelastic constitutive material model in frequency domain is used to define the micro-scale Representative Volume Element (RVE) of the studied composite biomaterial. The RVE simulates a fiber-reinforced composite with axonal fibers and extracellular glial. Each RVE is a representation of a continuum element in the compound material model of the BWM. Since the mechanical properties of the axons and the glial in the BWM are noticeably different, an RVE composed axonal fibers and extracellular glial is developed. Figure 1, to study the anisotropic viscoelastic properties in the frequency domain.

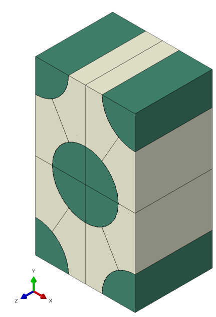

Fig. 1 Biphasic model (RVE) is a representation of white matter where a central axon surrounded by glial matter with another axon at the corners of the RVE. It allows for different packing geometries and for varying surface interaction at axon/glial interface [4]

The axon/glial VF ratio for the composite material is considered a representative property of the RVE along with the respective anisotropic material properties that stem from the geometric locations and tortuosity of axons in the glial. The frequency domain viscoelastic data was collected from both tensile and pure shear test performed on the RVEs with VFs in the range of 5%~85%. The frequency viscoelastic properties are expressed as storage modulus and loss modulus for the axon/glial composite structure. The RVE is subjected to tensile and pure shear tests in three different directions in order to identify per [4] its orthotropic viscoelastic properties in frequency domain, as described in Eq. (1). As seen E_{ij}, G_{ij}, ν_{ij} are the Young’s modulus, shear modulus and Poisson’s ratio in different material orientations as indexed by ij, $LC(VF)$ is the loss moduli compliance tensor, and $SC(VF)$ is the storage moduli compliance tensor. Different VFs will result in different loss and storage modulus compliance tensors.

$$LC(VF) = \begin{bmatrix} \frac{1}{E_{11}^L} & -\frac{\nu_{21}^L}{E_{22}^L} & -\frac{\nu_{31}^L}{E_{11}^L} & & & \\ -\frac{\nu_{12}^L}{E_{11}^L} & \frac{1}{E_{22}^L} & -\frac{\nu_{32}^L}{E_{33}^L} & & & \\ -\frac{\nu_{13}^L}{E_{11}^L} & -\frac{\nu_{23}^L}{E_{22}^L} & \frac{1}{E_{33}^L} & & & \\ & & & \frac{1}{G_{23}^L} & & \\ & & & & \frac{1}{G_{13}^L} & \\ & & & & & \frac{1}{G_{12}^L} \end{bmatrix}_{VF}, \tag{1}$$

$$SC(VF) = \begin{bmatrix} \frac{1}{E_{11}^S} & -\frac{\nu_{21}^S}{E_{22}^S} & -\frac{\nu_{31}^S}{E_{11}^S} & & & \\ -\frac{\nu_{12}^S}{E_{11}^S} & \frac{1}{E_{22}^S} & -\frac{\nu_{32}^S}{E_{33}^S} & & & \\ -\frac{\nu_{13}^S}{E_{11}^S} & -\frac{\nu_{23}^S}{E_{22}^S} & \frac{1}{E_{33}^S} & & & \\ & & & \frac{1}{G_{23}^S} & & \\ & & & & \frac{1}{G_{13}^S} & \\ & & & & & \frac{1}{G_{12}^S} \end{bmatrix}_{VF}, \tag{2}$$

The constitutive relationship of RVEs can be expressed as [4]:

$$\varepsilon(VF) = \big(SC(VF) + iLC(VF)\big)\sigma(VF), \tag{3}$$

where $i = \sqrt{-1}$ represents the imaginary axis of the complex variable, $\varepsilon(VF)$ and $\sigma(VF)$ are strain and stress with related VF.

2. *BWM model*

The BWM model comprises of a sophisticated compilation of RVEs that are combined to represent the region of the white matter under investigation. Although the combination of the RVEs is not unique the resulting properties and architectures of the homogenized BWM should accurately emulate the properties the targeted region. The BWM model inherits the material properties of the RVEs and then combines their orientation information to build the whole structure. The axonal tract orientation data are collected from 3D experimental tests. The overall longitudinal lengths (end-to-end length) of axonal traces are 30 μm for every axonal tract [13]. However, the arc lengths of the axons are different and can be calculated based on the 3D geometric data of the axonal traces. For an undulated axon, the tortuosity, *T*, is defined as the ratio of the arc length and end-to-end length of axon [2], which is a very important parameter for evaluating strain level of axons:

$$T = \frac{L_{arc}}{L_{end}}. \tag{4}$$

The BWM microscale computational models developed by Pelegri's group include discrete axons with tortuous paths and were coded using finite elements (FE) [2,3,4]. However due to the complexity of the internal structure of BWM, the axonal traces may have an irregular location in the extracellular glial, thus challenging the accurate representation of the BWM's geometric details by FEM. Especially, when the axons are in close proximity, the meshing capabilities of FEM often fail to capture the complexity and irregular geometry of the structure in a computationally efficient manner. Therefore, mesh generation needs to be cautiously redefined in the small region manually to avoid low-quality mesh which would cause structural failure or distortion.

3. *Material Orientation Computation*

Material orientation is based on the geometry of 3D axonal trace position data. Since the original 3D axonal position data are discretized points in 3D space, further processes are adopted to extract more information. First, discrete local coordinates were connected to build completed axon fibers by using a curve fitting algorithm in Abaqus. Then, the numerical values of tangents were extracted from the axonal traces based on target points on each tract. The tangents values are needed to specify the material orientation at the center of the RVE, see Fig. 2.

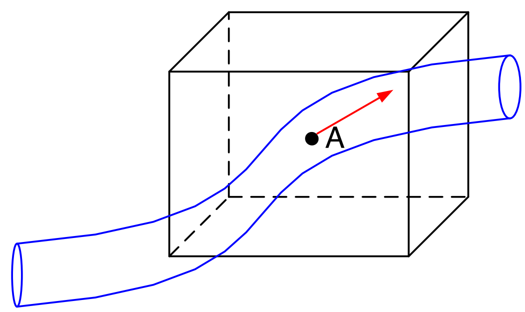

Fig. 2 Schematic of the orientation determination process. The blue part is a virtual example of an axon. The black cuboid is one of the finite element in a specific mesh size. The black point A is the center of this element. The red arrow is the tangent from the rebuilt axonal trace at the center point of this element. The red arrow will represent the material orientation for this element. The VF of this specific element can be computed out using intersection calculation methods.

In this study, the 3D Radial Basis Function (RBF) interpolation method is used to generate material orientation for every element. The RBF interpolation is based on computing the distance of two points in n-dimensional space and is defined by a function [14,15]:

$$f(\boldsymbol{x}) = \sum_i^N \lambda_i \phi(r_i) = \sum_i^N \lambda_i \phi(\|\boldsymbol{x} - \boldsymbol{x}_i\|_2) \tag{5}$$

where $r_i = \|\boldsymbol{x} - \boldsymbol{x}_i\|_2 = \sqrt[2]{(x - x_i)^2 + (y - y_i)^2 + (z - z_i)^2}$ is the distance between $\boldsymbol{x}$ and $\boldsymbol{x}_i$ for ith point, $\boldsymbol{x} = (x, y, z)$ are coordinate locations in 3D space, λ_i is weight to be computed, and $\phi(r_i)$ is RBF. For a given data set (x_i, h_i), where h_i are the associated values to be interpolated and x_i are the point coordinates, input the set (x_i, h_i) into the function *f(x)* of Eq. (5) to solve the linear system and obtain the weight λ_i in the interpolation function. The methodology to compute the material orientation based on the RBF interpolation method is described hereafter.

First, numbers of the points and related tangents of each axonal tract are selected as the input training data of the 3D-RBF interpolation. The tangents have three different direction components (h_i^x, h_i^y, h_i^z for x, y, z directions in 3D space) so that the input training data will be separated as 3 parts for 3 RBF interpolation functions in 3 material orientations. Second, the center points of every element of the data are tested and result in 3 different directional components, which are sequentially combined to identify the final material orientation on every element. After those two processes, every element in the BWM model has their own material orientation computed based on RBF interpolation. Comparing our data set with different Radial Basis Functions, concluded that the linear distant RBF $\phi(r_i) = r_i$ performs better than other methods in our study.

ANALYSIS AND RESULT

In this simulation, the location coordinates of two axonal traces in 3-D space are selected as the input information [3]. The geometry of the axonal traces can be generated using the spline function in ABAQUS. The tortuosity of two axonal traces is calculated from the Eq. (4) as 1.12 and 1.19. The two axons are denoted by the red splines in the Fig. 3 in which the axonal traces' locations and directions are virtually displayed.

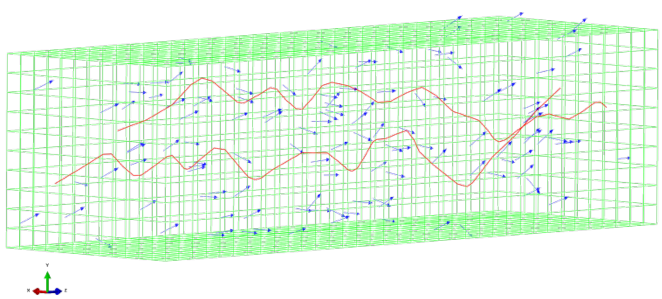

Fig. 3 BWM depicting 2 axonal splines and material orientation in 3D space. There are 4320 elements of size 20*20*20 µm each in the BWM model. The red splines are axonal traces generated from axonal location coordinate data. The material orientations in local axonal direction are indicated by the blue arrows on the elements that are generated from RVE. All 4320 elements have material orientations inferred by 3D-RBF methods. For clarity, only a small part of the elements were selected to illustrate the orientations in the BWM model.

An FE model representing the axon/glia RVE assemblies as described by the orientation and location of the axonal traces will the developed using ABAQUS 6.14 and Python scripting. As shown in Fig. 3, the BWM model is built by 4320 elements in total. The internal elements' grids are hidden in order to reveal clear structure view inside the BWM model. The material orientations indicated by blue arrows precisely follow the axonal traces' direction denoted by the red splines. As noted in Fig. 3 the BWM includes the RVE material properties, axonal trace directions, and axonal tortuosity information to depict a more realistic simulation tool for white matter contrasting the current straight fiber models presented in literature.

In addition, VF of all part of BWM model was 65%. Each element has the same edge length of $20\mu m$. The virtual axonal radius in RVE is $15\mu m$. The original material properties of axon and glial used in this study are shear storage/loss moduli in the frequency of 50Hz [15] where $G_{axon}^{storage} = 2.15kPa$, $G_{axon}^{loss} = 1.75kPa$, $G_{glial}^{storage} = 0.85kPa$, and $G_{glial}^{loss} = 0.3kPa$. The Poisson ratio is assumed $\nu = 0.49$ following the incompressibility assumption for soft tissue. According to the above material properties, the orthotropic storage and loss moduli compliance tensors, SMCT and LMCT respectively, can be calculated based on Eq. (1) and Eq. (2). The calculated LMCT and SMCT will be consecutively used as input data to the RVE model [16]. The orthotropic, frequency dependent, viscoelastic properties will then be obtained from Eqs. (1-2) and will be the material properties assigned to the BWM model.

Figure 4 elucidates the results of the analysis for stress magnitudes and directions of the BWM model subjected to harmonic excitation loading at the 50Hz frequency with 0.01 tensile strains in the Z-direction. The result clearly portrays the direction of local complex maximum principal stresses following the axonal traces' direction. The highest stresses magnitude region of the real component of the complex maximum principal stress in Fig. 4 (a) is concentrated in the central area of BWM model. Conversely, in Fig. 4 (b), the highest stresses magnitude region of the imaginary component of the complex maximum principal stress is focused on boundary of the positive Z- and negative Z-directions. Figures 4 (a)-(b) illustrate that the stress magnitude and direction changes are highly related to the axons' direction and tortuosity gradients.

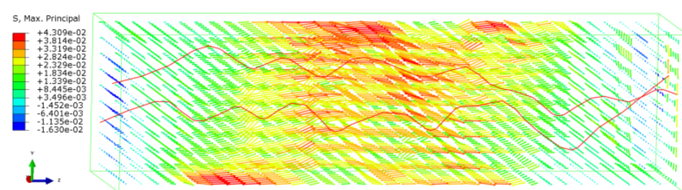

(a)

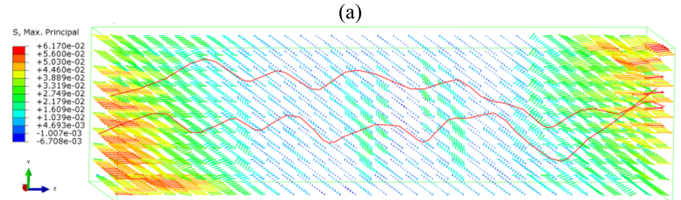

(b)

Fig. 4 BWM model with varying material orientation analysis result of complex maximum principal stress (unit is kPa) under harmonic excitation of 0.01 tensile strain at 50Hz in the Z-direction of (a) real component of complex maximum principal stress and (b) imaginary component of complex maximum principal stress. The red spline is the virtual axon denoting the axonal traces direction and location. The different color arrows indicate the stress magnitudes and directions in the local coordinates of each element.

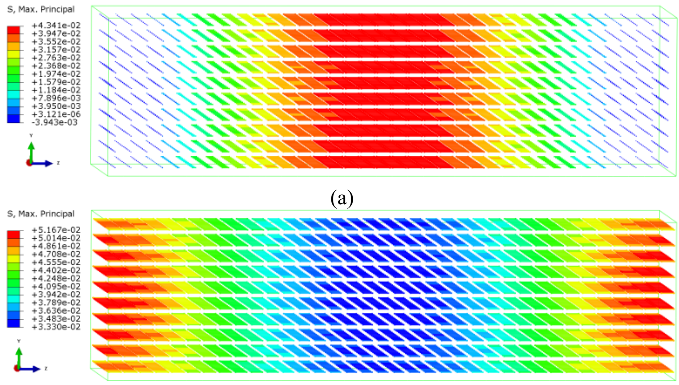

Fig. 5 BWM model with identical material orientation analysis result of complex maximum principal stress (unit is kPa) under harmonic excitation of 0.01 tensile strains loading at the 50Hz frequency steady state dynamic analysis in Z direction of (a) real component of complex maximum principal stress and (b) imaginary component of complex maximum principal stress.

In order to study the importance of orientation information in the BWM model an additional simulation was run in which the material properties and material orientations were the same in every element. Figure 5 shows the results of the above mentioned simulation. As seen, the maximum principal stress is identical in all of BWM elements. Comparing the result of Figs 4-5, it is clear that the axonal tortuosity has a significant effect on the material response and an important impact on the steady state dynamic analysis results of the composite BWM model. That means material orientation should be a very important consideration in further analysis of BWM.

CONCLUSION

In this study, a BWM FE model was built based on merging RVE material properties, volume fractions, and material orientation information. The BWM model yields clear prediction on stress magnitude and direction changes resulting from 50Hz frequency at steady state dynamic analysis. The stress magnitude and direction were shown to be strongly influenced by the axonal trace location and the tortuosity change when subjected to tension. In conclusion, this model offers a method to calculate the response of a real BWM tissue based on its nanoscale architecture and it's a first step in corelating nanoscale studies with MRI and MRE which are larger scale diagnostic modalities.

ACKNOWLEDGMENTS

The authors would like to kindly acknowledge the support of NSF CMMI-1763005 - 823794 award.

REFERENCES

[1] Singh, Sagar. "Modeling methods in understanding and ameliorating central nervous system injury." PhD diss., Rutgers University-Graduate School-New Brunswick, 2016

[2] Pan, Yi, David I. Shreiber, and Assimina A. Pelegri. "A transition model for finite element simulation of kinematics of central nervous system white matter." IEEE Transactions on Biomedical Engineering 58, no. 12 (2011): 3443-3446.

[3] Yi Pan, Pan, Yi, Daniel Sullivan, David I. Shreiber, and Assimina A. Pelegri. "Finite element modeling of CNS white matter kinematics: use of a 3D RVE to determine material properties." Frontiers in bioengineering and biotechnology 1 (2013): 19.

[4] Daniel Sullivan, Assimina Pelegri, "A Finite Element Approach to Finding the Anisotropic Viscoelastic Properties of Tied and Untied Axonal White Matter for Magnetic Resonance Elastography", Technical Presentation, IMECE2017-72644.

[5] Javid, Samad, Asghar Rezaei, and Ghodrat Karami. "A micromechanical procedure for viscoelastic characterization of the axons and ECM of the brainstem." Journal of the mechanical behavior of biomedical materials 30 (2014): 290-299.

[6] Abolfathi, Naik, A. Naik, M. Sotudeh Chafi, G. Karami, and M. Ziejewski. "A micromechanical procedure for modelling the anisotropic mechanical properties of brain white matter." Computer Methods in Biomechanics and Biomedical Engineering 12, no. 3 (2009): 249-262.Javid, Samad, Asghar Rezaei, and Ghodrat Karami. "A micromechanical procedure for viscoelastic characterization of the axons and ECM of the brainstem." Journal of the mechanical behavior of biomedical materials 30 (2014): 290-299.

[7] Feng, Yuan, Ruth J. Okamoto, Ravi Namani, Guy M. Genin, and Philip V. Bayly. "Measurements of mechanical anisotropy in brain tissue and implications for transversely isotropic material models of white matter." Journal of the mechanical behavior of biomedical materials 23 (2013): 117-132.

[8] Colgan, Niall C., Michael D. Gilchrist, and Kathleen M. Curran. "Applying DTI white matter orientations to finite element head models to examine diffuse TBI under high rotational accelerations." Progress in biophysics and molecular biology 103, no. 2-3 (2010): 304-309.

[9] Cloots, R. J. H., J. A. W. Van Dommelen, and M. G. D. Geers. "A tissue-level anisotropic criterion for brain injury based on microstructural axonal deformation." Journal of the mechanical behavior of biomedical materials 5, no. 1 (2012): 41-52.

[10] Sullivan, Sarah, Stephanie A. Eucker, David Gabrieli, Connor Bradfield, Brittany Coats, Matthew R. Maltese, Jongho Lee, Colin Smith, and Susan S. Margulies. "White matter tract-oriented deformation predicts traumatic axonal brain injury and reveals rotational direction-specific vulnerabilities." Biomechanics and modeling in mechanobiology 14, no. 4 (2015): 877-896.

[11] Sahoo, Debasis, Caroline Deck, and Rémy Willinger. "Development and validation of an advanced anisotropic visco-hyperelastic human brain FE model." journal of the

mechanical behavior of biomedical materials 33 (2014): 24-42.

[12] Findley, William N., and Francis A. Davis. Creep and relaxation of nonlinear viscoelastic materials. Courier Corporation, 2013.

[13] Singh, Sagar, Assimina A. Pelegri, and David I. Shreiber. "Characterization of the three-dimensional kinematic behavior of axons in central nervous system white matter." Biomechanics and modeling in mechanobiology 14, no. 6 (2015): 1303-1315.

[14] Skala, Vaclav. "RBF interpolation with CSRBF of large data sets." Procedia Computer Science 108 (2017): 2433-2437.

[15] Fornberg, Bengt, and Natasha Flyer. "Accuracy of radial basis function interpolation and derivative approximations on 1-D infinite grids." Advances in Computational Mathematics 23, no. 1-2 (2005): 5-20.

[16] Arbogast, Kristy B., and Susan S. Margulies. "A fiber-reinforced composite model of the viscoelastic behavior of the brainstem in shear." Journal of biomechanics 32, no. 8 (1999): 865-870.